Iranian Journal of Medical Physics
Vol. 13, No. 3, September 2016, 211-217
Received: May 10, 2016; Accepted: July 02, 2016

Original Article

Developing the Adult Male ICRP Phantom and Evaluation the Absorbed Dose Received By Critical Organs in Head and Neck Region during the Radiotherapy of Eye Cancer

Alireza Vejdani-Noghreiyan[1], Atiyeh Ebrahimi-Khankook[1*]

Abstract

Introduction
Accurate estimation of the absorbed dose in radiosensitive organs, located away from the target volume during radiotherapy, is one of the main reasons for the development of reference phantoms. The International Commission on Radiological Protection (ICRP) reference phantoms can provide a more realistic view of the human anatomy in comparison with the previously used mathematical phantoms. However, the ICRP reference phantoms seem to have certain limitations, resulting in the inaccurate eye simulation due to the absence of super-high-resolution CT scan images.
Materials and Methods
In this study, we developed a modified version of the ICRP reference phantom by inserting a realistic eye phantom into the voxelized phantom. In addition, by using the developed model, the absorbed dose received by sensitive organs (e.g., thyroid, brain, and different parts of the eye) during radiotherapy of a common ocular surface tumor was determined. The results were compared with those obtained by the modified phantom developed by the University of Florida-Oak Ridge National Laboratory (UF-ORNL).
Results
Based on the results, the relative difference between the equivalent doses calculated by the developed phantom and UF-ORNL phantom was nearly 75-95% and 3% for thyroid and eye substructures, respectively.
Conclusion
Despite of many advantageous of voxel phantoms, they have considerable limitation in providing accurate model of the eye. In the present study, a detailed stylized model was developed and incorporated into the Adult Male (AM) reference and UF-ORNL phantoms. These phantoms were then used for the dosimetric calculations during eyelid cancer therapy.

Keywords: Dosimetry, Eye, Mathematical model, Radiotherapy

1- Physics Department, Faculty of Sciences, University of Neyshabur, Neyshabur, Iran,

*Corresponding author: Tel: +98 514-330-5000; Fax: +98-514-330-5234; E-mail:at_ebrahimi65@yahoo.com

1. Introduction

Computerized treatment planning systems (TPSs) are CT-based tools, widely used in radiotherapy centers. However, these systems lack sufficient accuracy for detailed modeling of the elemental composition and density of different tissues. In these cases, calculations performed by TPSs do not provide an accurate estimation of the absorbed dose of radiosensitive organs, located outside the target volume; consequently, they should be corrected using Monte Carlo calculations [1].

Over the past decade, computational models of the human anatomy have been widely used in dosimetric calculations [2-5]. The advent of tomographic imaging techniques has facilitated the construction of digital three-dimensional models, based on the real anatomy of the human body [6, 7]. Compared with mathematical phantoms, voxelized phantoms, which are developed based on CT and MRI images, provide a much more realistic view of the human anatomy [8, 9].

In radiotherapy, partial-body patient phantoms are mostly constructed using a series of CT or MRI images obtained from the target region of the patient. However, in practice, development of a whole-body patient-specific phantom (WBPP) is quite challenging and time-consuming. Therefore, when the immediate estimation of the absorbed dose is required for radiosensitive organs away from the target volume, the standard reference phantoms are profitable [9-11].

The International Commission on Radiological Protection (ICRP) has developed reference computational phantoms of adult males and females, which are consistent with the external dimensions, organ masses, and tissue data of standard man and woman [12]. This set of adult phantoms can be used for the accurate estimation of the received dose by organs away from the target volume [9, 13-15].

It is obvious that the data obtained by WBPP is more accurate. However, since the construction of WBPP is a time-consuming procedure requiring whole-body CT data of the patient, a standard reference phantom as an auxiliary tool can be significant and profitable.

It is worth mentioning that the anatomical realism of voxelized phantoms makes them preferable as the standard model in comparison with mathematical models. However, voxelized phantoms have limitations in the accurate segmentation of different parts of the human eye with different levels of sensitivity to radiation [12, 16].

Considering the radiosensitivity of some parts of the human eye, details of the human eye anatomy should be considered in the anatomical simulation. Previously, Nogueira et al. and Behrens et al. reported the details of the human eye anatomy, using surface equations [17, 18]. In this study, the adult male ICRP reference phantom was developed by inserting a mathematical realistic phantom of the eye. In addition, by using the developed model, the absorbed dose of sensitive organs, such as thyroid, brain, and different parts of the eye, was determined during radiotherapy of a common ocular surface tumor.

2. Materials and Methods

This study was done by the support provided by the Vice-chancellor for Research and Education at the Nuclear Simulation Laboratory of University of Neyshabur, Iran. The required information about the anatomical structure of the human eye was extracted from previous studies performed by Behrens et al. and Nogueira et al. [17, 18]. Different substructures of the realistic eye model used in this study are illustrated in Figure 1.

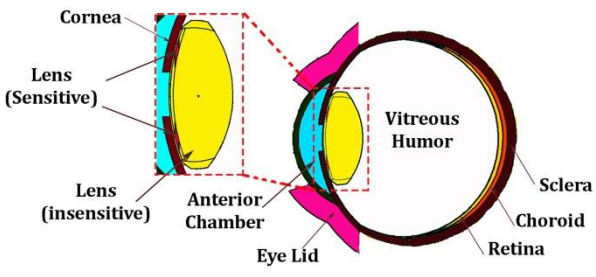

Figure 1. Different substructures of the eye

In addition, Figure 2a shows the equations which describe the geometrical shape of different structures of the modified left eye.

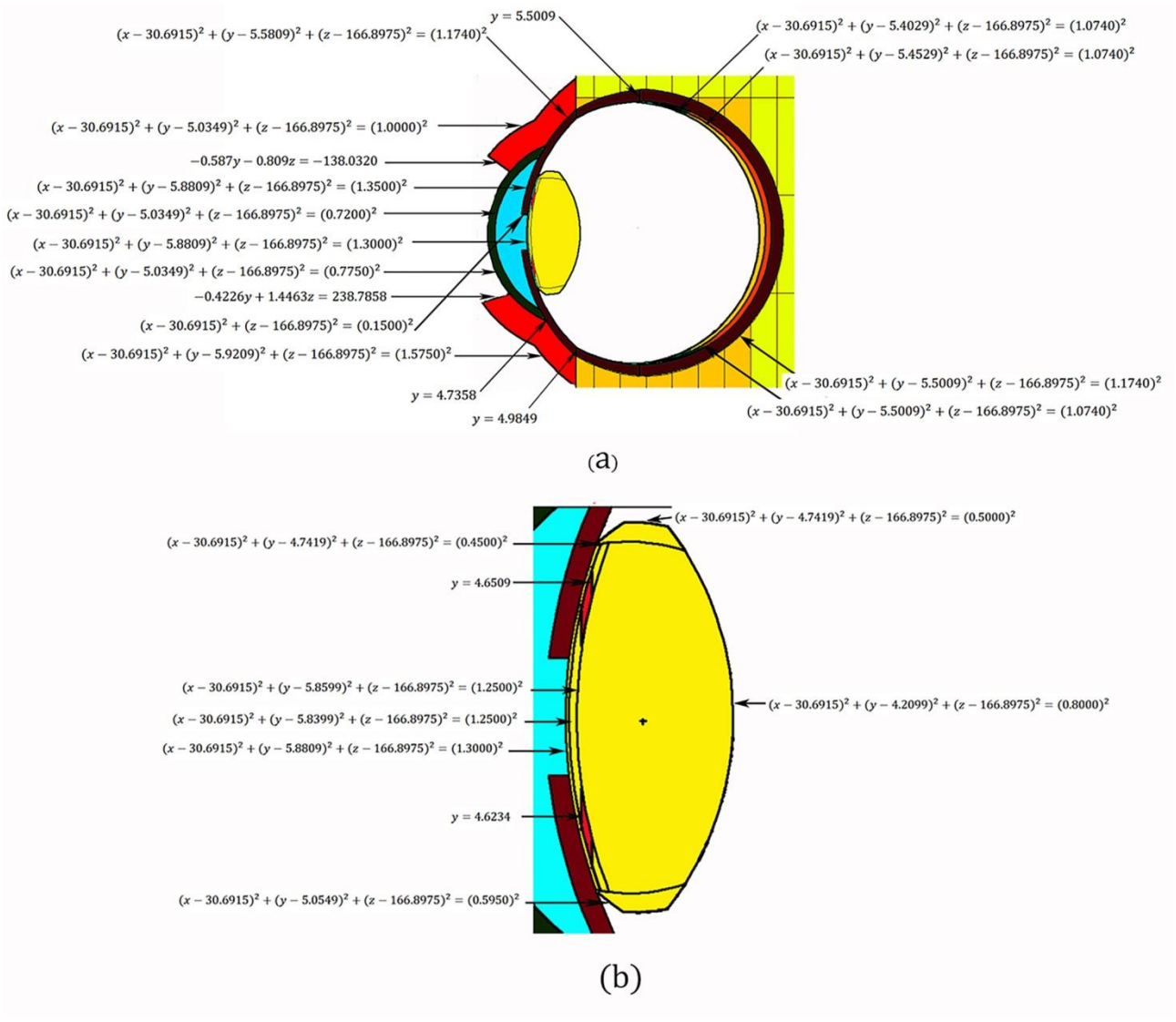

Figure 2. (a) Modified eye model being compatible with AM phantom. The equations given describe the various structures of the left eye. (b) Close view of the human eye lens.

A close view of the lens substructures and the related equations is also presented in Figure 2b (all dimensions are in centimeter). In addition, Figure 3 presents a three-dimensional view of the modified eye model before insertion into the Adult Male (AM) phantom; different parts of the eye are also shown in this figure.

To illustrate the necessity of using the developed voxelized phantom, the realistic eye phantom was also incorporated into the UF-ORNL mathematical phantom. Both models were used to estimate the dose delivered to different parts of the eye and other sensitive organs in the head and neck regions during eye cancer radiotherapy [19].

A mid-size tumor (3 mm in diameter) was simulated on the lid of the left eye. Then, the received doses by the brain, thyroid, and different parts of the eye were calculated when the tumor was exposed to a 5×5 cm^2 field of photon and electron irradiation. The developed phantoms were implemented in MCNPX 2.6.0 code [20]. In total, eight different photon and electron energies were investigated, and the doses received by different parts of the eye were estimated. Moreover, the delivered doses to the brain and thyroid of the modified UF-ORNL and reference phantoms were compared as the lid tumor was irradiated.

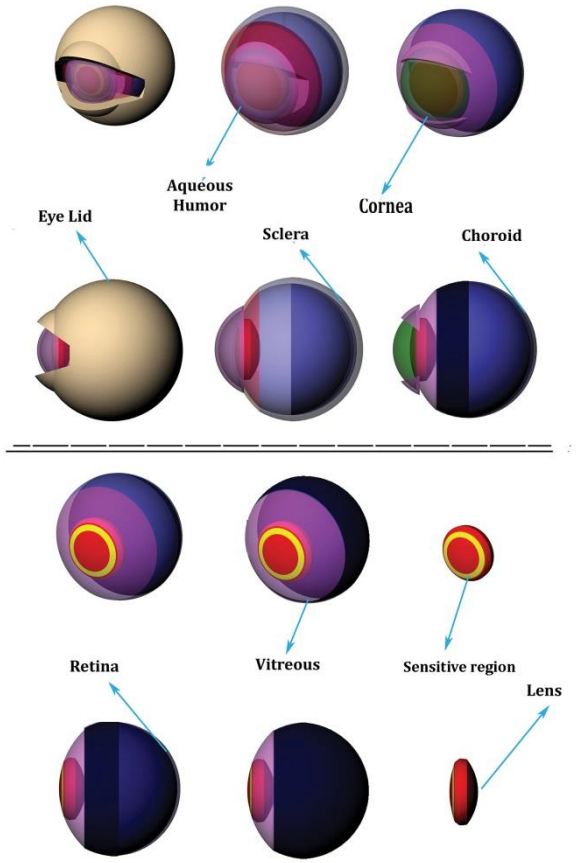

Figure 3. 3D view of the eye model simulated in this work

To simulate the photon sources, the output spectra of Clinac-4 (4 MV), Clinac-6 (6 MV), Clinac-18 (10 MV), and Clinac-20 (15 MV) were simulated, using the data reported by Mohan and colleagues [21]. Also, to simulate the electron sources, the energy spectra of 7, 8, 9, and 10 MeV output electrons from LIAC and NOVAC linear accelerators were simulated [22].

For such evaluations, secondary particles were tracked and the organ absorbed doses were computed, using a collision heating tally (+F6). To calculate the equivalent dose, the radiation weighting factor (w_R) was used to convert the physical dose (Gy) to photon and electron equivalent doses (Sv) [23].

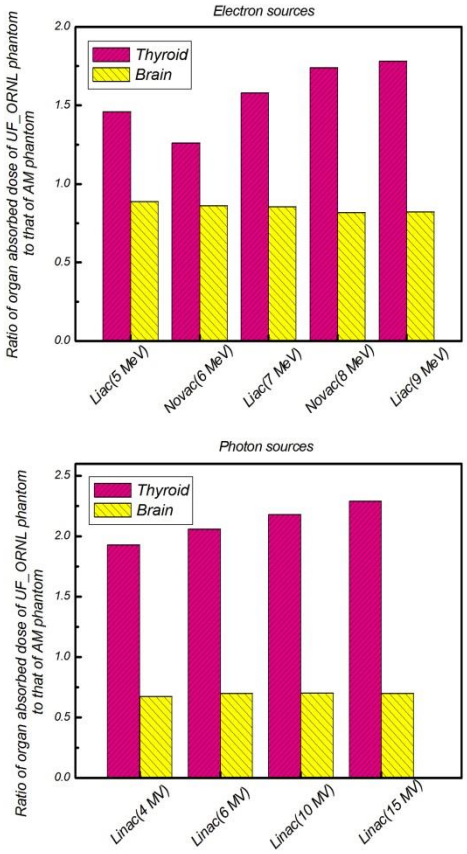

Figure 4. The ratio of the brain and thyroid equivalent doses of the UF-ORNL phantoms to that of the AM phantoms during exposing the tumor to (a) electron and (b) photon beams

3. Results

Table 1 shows the arithmetic mean of equivalent doses received by the eye substructures in the two investigated phantoms. The data was normalized by the minimum equivalent dose to tumor at 50 Sv, which is the treatment dose commonly used for ocular tumors [24]. Figure 4 presents the comparison between the dose received by the brain and thyroid, using the modified UF-ORNL and reference phantoms.

The estimated thyroid dose in the modified reference phantom was lower than the estimated dose received by thyroid in the modified UF-ORNL phantom. The relative differences were up to 75% and 95% for the electron and photon exposures, respectively. In addition, the relative difference in the brain dose was nearly30% for the electron exposure and about 10% for the photon exposure.

Table 1. Equivalent dose for various substructures of the eye in Sv.

Energy	Lens			Cornea	Anterior Chamber	Vitreous Humor	Sclera	Retina	Choroid
	Sens. Re.	Insens. Re.	Total						
Photon Beams									
4 MV	15.81	19.11	19.05	22.49	16.03	42.06	47.78	44.8	45.05
6 MV	19.89	23.36	23.29	20.34	18.92	50.06	56.01	55.27	55.37
10 MV	22.16	26.3	26.21	24.29	20.36	56.56	62.92	66.24	67.07
15 MV	24.38	29.12	29.02	26.20	22.58	59.51	65.92	71.08	71.68
Electron Beams									
7 MeV	3.33	4.92	4.90	12.36	6.42	18.78	23.31	19.96	19.76
8 MeV	3.02	4.48	4.46	12.43	6.35	18.28	22.99	19.75	19.69
9 MeV	2.93	4.31	4.28	12.13	6.03	18.46	23.30	20.32	20.19
10 MeV	2.03	3.41	3.39	11.87	5.42	17.82	22.98	20.05	20.02

Table 2 Statistical indices of distributions of the relative differences between the considered organ and tumor

Phantom	Organ	Mean	Standard Deviation	Skewness	Kurtosis
UF-ORNL	Brain	10.79	3.43	-0.106	-0.729
	Thyroid	14.74	1.24	-0.031	-0.916
AM	Brain	11.19	3.39	-0.261	-0.725
	Thyroid	20.67	1.00	-0.406	-1.910

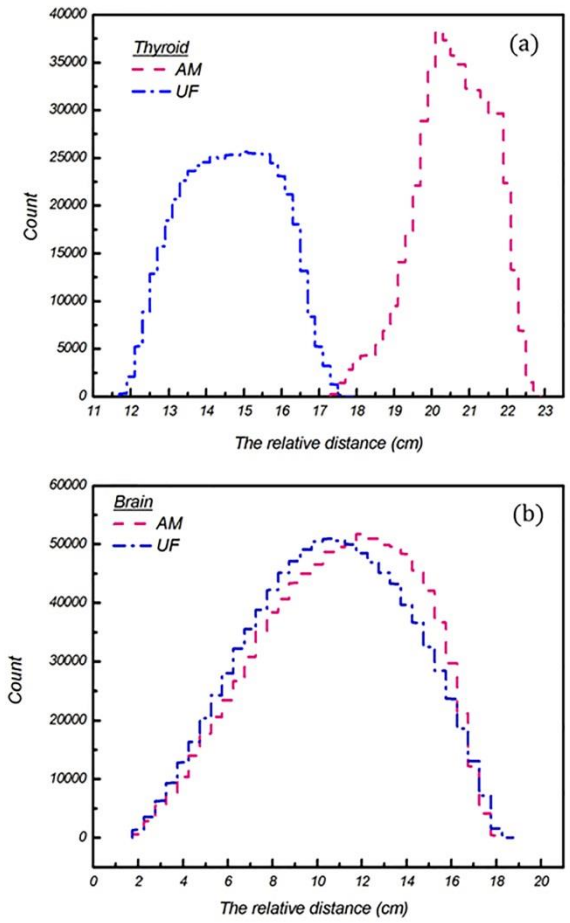

Figure 5. The relative distances of brain from the target region (RDB) and the relative distances of thyroid from the target volume (RDT) in two phantoms

In order to investigate the differences between the doses received by critical organs in UF-ORNL and AM phantoms, the relative distances between these organs and the target region were calculated. Figure 5a indicates the distribution of the relative distance between two points, randomly sampled in the tumor and thyroid, respectively.

The distribution was evaluated for one million random points. A similar distribution was provided for the brain, as demonstrated in Figure 5b. Since the points were sampled normally, the relative distance between the points was expected to have a normal distribution. The normality of these distributions was analyzed by calculating the kurtosis and skewness of these distributions, using SPSS version 20 (IBM SPSS Inc., Chicago, IL, USA).

Table 2 indicates the statistical indices of the distributions presented in Figure 5. It can be observed that skewness and kurtosis were very close to zero; therefore, the statistical analysis confirmed the normality of these distributions.

4. Discussion

The arithmetic means of the received dose by eye substructures in UF-ORNL and AM phantoms are presented in Table 1. As demonstrated in this table, the vitreous humor,

sclera, choroid, and retina received greater doses in comparison with other parts of the eye due to their relative positions with respect to the irradiation field.

Figure 4 compares the dose received by the brain and thyroid in the two investigated phantoms. Accordingly, the brain in UF-ORNL phantom received a lower dose than the AM phantom. The difference varied from about 10% for photon exposures to 30% for electron beams.

However, the thyroid dose of UF-ORNL phantom was considerably higher than that of the AM phantom (> 70%). These variations can be explained by the differences between the relative distance of the brain and thyroid from the target region in two phantoms. As shown in this figure, thyroid and brain in the UF-ORNL phantom were closer to the tumor which is why the brain and thyroid doses in this phantom were greater than the reference phantom. Since thyroid was farther away from the target volume than the brain, the difference in thyroid dose was much higher than that of the brain.

Combination of the voxelized reference and UF-ORNL phantoms with the realistic model of the eye facilitates the simultaneous estimation of doses delivered to different parts of the eye and other sensitive organs in the head and neck regions. However, due to differences in the organ shape and position, the results of two phantoms were not similar.

The phantoms could provide an approximate estimation of the upper and lower limits of the dose delivered to the organs which are far from the target volume and cannot be simulated in the partial-body specific phantom. Since the ICRP reference phantom is preferable to UF-ORNL phantom for cases which require more anatomical details, use of data obtained from the AM phantom is suggested.

5. Conclusion

In this study, a realistic mathematical model of the eye was incorporated into the AM and UF-ORNL phantoms to investigate the possibility of determining ocular damages and simultaneously estimate the delivered dose to critical organs in the head and neck regions. The results of the photon and electron therapies of a typical lid cancer were studied by using the modified UF-ORNL and reference phantoms. Despite the similar dose data obtained by these two phantoms for eye substructures, there were considerable differences between the thyroid and brain doses for the two phantom sets. Therefore, to estimate the dose delivered to the organs, which are not accurately represented in the mathematical phantom, use of an ICRP phantom can be profitable. In addition, for organs simulated in both phantoms, an approximate estimation of the upper and lower limits of the dose was presented.

Acknowledgements

The authors would like to acknowledge the support of the Vice-chancellor for research and education of University of Neyshabur.

References

1- Ghorbani M, Tabatabaei Z, VejdaniNoghreiyan A, SoleimaniMeigooni A.Evaluation of Tissue Composition Effect On Dose Distribution in Radiotherapy with 6 MV Photon Beam of a Medical Linac. 57th Annual Meeting &Exhibition, Anaheim;2015; California, USA.

2- Assar E, Motavalli LR, Miri-Hakimabad H, Vejdani-Noghreiyan A. The operator dose assessment of landmine detection systems using the neutron backscattering method. J. Radioanal. Nucl. Chem.2013;298:375-81.DOI: 10.1007/s10967-013-2501-3.

3- Mohammadi N, Miri-Hakimabad H, Rafat-Motavalli L, Akbari F, Abdollahi S. Patient-specific voxel phantom dosimetry during the prostate treatment with high-energy linac. J. Radioanal. Nucl. Chem.2014;304:785-92.DOI: 10.1007/s10967-014-3872-9.

4- Zaidi H, Tsui BM. Review of computational anthropomorphic anatomical and physiological models. Proceedings of the IEEE.2009; 97:1938-53.DOI: 10.1109/JPROC.2009.2032852.
5- Jabbari I, Shahriari M, Aghamiri SM, Monadi S. Advantages of mesh tallying in MCNPX for 3D dose calculations in radiotherapy. J. Radioanal. Nucl. Chem. 2012; 291: 831-7.DOI: 10.1007/s10967-011-1393-3.
6- Caon M. Voxel-based computational models of real human anatomy: a review. Radiat.Environ.Biophys.2004; 42:229-35.DOI: 10.1007/s00411-003-0221-8.
7- Caon M, Mohyla J. Automating the segmentation of medical images for the production of voxel tomographic computational models. Australas. Phys. Eng. Sci. Med.2001; 24:185-90. DOI: 10.1007/BF03178363.
8- Saito K, Wittmann A, Koga S, Ida Y, Kamei T, Funabiki J, Zankl M. Construction of a computed tomographic phantom for a Japanese male adult and dose calculation system. Radiat.Environ.Biophys. 2001; 40:69-76.DOI: 10.1007/s004110000082.
9- Xu XG. Computational phantoms for radiation dosimetry: A 40-year history of evaluation. In: Handbook of anatomical models for radiation dosimetry. London Newyork: CRC Press. 2009:3-35.
10- Hadid L, Desbrée A, Schlattl H, Franck D, Blanchardon E, Zankl M. Application of the ICRP/ICRU reference computational phantoms to internal dosimetry: calculation of specific absorbed fractions of energy for photons and electrons. Phys. Med. Biol. 2010; 55: 3631-41.DOI: 10.1088/0031-9155/55/13/004.
11- Kim CH, Jeong JH, Bolch WE, Cho KW, Hwang, SB. A polygon-surface reference Korean male phantom (PSRK-Man) and its direct implementation in Geant4 Monte Carlo simulation. Phys. Med. Biol. 2011; 56: 3137-61.DOI: 10.1088/0031-9155/56/10/016.
12- ICRP Publication 110.Adult reference computational phantom. Ann. ICRP 39 (2), 2009.
13- Endo A, Petoussi-Henss N, Zankl M, Bolch WE, Eckerman KF, HertelNEet al. Overview of the ICRP/ICRU adult reference computational phantoms and dose conversion coefficients for external idealised exposures. Radiat. Prot.Dosim. 2014; 161:11-6.DOI: 10.1093/rpd/nct304.
14- Schlattl H, Zankl M, Petoussi-Henss N. Organ dose conversion coefficients for voxel models of the reference male and female from idealized photon exposures. Phys. Med. Biol. 2007; 52:2123-45.DOI: 10.1088/0031-9155/52/8/006.
15- ICRP Publication 116.Conversion coefficients for radiological protection quantities for external radiation exposures. Ann. ICRP 40(2-5), 2010.
16- Charles MW, Brown N. Dimensions of the human eye relevant to radiation protection (dosimetry). Phys.Med.Biol.1975;20:202-18.DOI: 10.1088/0031-9155/20/2/002.
17- Behrens R, Dietze G, Zankl M. Dose conversion coefficients for electron exposure of the human eye lens. Phys. Med. Biol.2009; 54:4069-87.DOI: 10.1088/0031-9155/54/13/008.
18- Nogueira P, Zankl M, Schlattl H, Vaz P. Dose conversion coefficients for monoenergetic electrons incident on a realistic human eye model with different lens cell populations. Phys. Med. Biol.2011; 56:6919-34.DOI: 10.1088/0031-9155/56/21/010.
19- Han EY, Bolch WE, Eckerman KF. Revisions to the ORNL series of adult and pediatric computational phantoms for use with the MIRD schema. Health. Phys. 2006; 90:337-56.DOI: 10.1097/01.HP.0000192318.13190.c4.
20- Hendricks JS, McKinney GW, Waters LS. MCNPX User's Manual, version 2.5. 0. Los Alamos National Laboratory. 2005.
21- Mohan R, Chui C, Lidofsky L. Energy and angular distributions of photons from medical linear accelerators. Med. Phys. 1985; 12:592-7.DOI: 10.1118/1.595680.
22- Righi S, Karaj E, Felici G, Di Martino F. Dosimetric characteristics of electron beams produced by two mobile accelerators, Novac7 and Liac, for intraoperative radiation therapy through Monte Carlo simulation. J. Appl. Clin. Med. Phys. 2013; 14:1-17.DOI: 10.1120/jacmp.v14i1.3678.
23- Kane SA. Introduction to modern physics. CRC Press, Taylor & Francis Group. 2009.
24- Muller K, Nowak PJ, de Pan C, Marijnissen JP, Paridaens DA, Levendag Pet al. Effectiveness of fractionated stereotactic radiotherapy for uveal melanoma. Int. J. Radiat. Oncol. Biol. Phys. 2005; 63: 116-22.DOI:10.1016/j.ijrobp.2005.01.058.